

# Hall transport in the topological non-Hermitian checkerboard lattice

Pedro G. de Oliveira<sup>a\*</sup> and Antônio S. T. Pires<sup>a</sup>

July 31, 2024

<sup>a</sup>*Department of Physics, Federal University of Minas Gerais, Belo Horizonte, MG, Brazil.*

<sup>\*</sup>*pgo.pedro@gmail.com*

## Abstract

The checkerboard lattice is a two-dimensional non-trivial structure usually seen as a planar version of the pyrochlore lattice. This geometry supports a two-band insulating electronic system with Chern topology induced by a complex hopping parameter. Inspired by the recent advances in the topology of non-Hermitian systems, in this work we study a non-Hermitian version of the topological checkerboard lattice. The complex band structure and Berry curvature are calculated. In the insulating phase, the Chern number is the same as in the Hermitian version, but the Hall conductivity is no longer quantized. The dependence of the Hall conductivity with the non-Hermitian parameters is investigated. The non-Hermiticity can be seen as a result of dissipation caused by coupling the system to the environment, so this study casts light on the topology of open systems in condensed matter physics.

## 1 Introduction

The study of condensed matter systems from a topological point of view has elucidated interesting novel phenomena in the last decades, the most famous example being the concept of topological insulators [1, 2]. The topological approach was fruitful in a variety of models, like magnetic, photonic, acoustic and superconducting systems [3–8]. While topological effects in regular, energy-conserving Hamiltonians is a established fact with robust theoretical and experimental evidence, that investigation in non-conservative open systems is still in progress. One way to model an open system is with a non-Hermitian Hamiltonian. The non-Hermitian formalism can be applied to a variety of quantum and classical systems, and the topology of non-Hermitian systems is an on-going field of study [9–13]. Specifically in fermionic systems, it is known that the non-Hermiticity spoils the bulk-edge correspondence of Chern topological insulators, and some efforts have been done to restore it [14]. Another consequence is that the Hall conductivity is no longer quantized [15–17]. For that reason, exploring the interplay between non-Hermiticity and topological effects on different platforms is a valuable way to elucidate the physics of open systems.

The checkerboard lattice is a nontrivial two-dimensional lattice structure with square geometry, which can be seen as a planar version of the pyrochlore

lattice [18–33]. The experimental realization is challenging, but the structure has already been discovered in some compounds [34–36]. The checkerboard lattice has some interesting properties. For instance, it is a member of a set of structures known as line-graph lattices, which show flat bands and spatially localized states [26, 27]. It has also been shown that it can hold variety of topological states [18, 20, 23–26, 28–33]. One interesting context to study these topological states is in a dissipative environment, which can be represented by a non-Hermitian Hamiltonian.

Motivated by the non-trivial topology of the fermionic checkerboard lattice, the main purpose of this work is to study a non-Hermitian version of this lattice, with a focus on the Hall transport and its response to the non-Hermitian parameters. This paper is organized as follows: in Section 2 we discuss the description of open quantum systems with non-Hermitian Hamiltonians. In section 3 we introduce the checkerboard lattice and show results for the fermionic Hermitian Hamiltonian. In Section 3 we introduce the non-Hermitian Hamiltonian and calculate its complex band structure. In Section 5 we calculate the system's Hall conductivity, and show how it varies in response to the non-Hermitian parameters. In Section 6 we summarize our findings.

## 2 Non-Hermitian Hamiltonian for open systems

Non-Hermitian Hamiltonians are a well-known way to describe open quantum systems, which present mechanisms of gain and loss of energy or particles. These open systems account for many physical processes, for instance, the interaction of a quantum system with a surrounding environment or an experimental apparatus of continuous measures [9]. Regarding the interaction of a two-band quantum system with its surroundings, one way to describe it is to locally couple the system to a series of baths (which represents the environment) [37]. That formalism accounts for a lossy system, where quasiparticles have finite lifetime due to dissipation. Integrating out the baths' degrees of freedom we obtain a Green function of the form  $G(\mathbf{k}, \epsilon) = (\epsilon - H(\mathbf{k}) - \Sigma(\mathbf{k}, \epsilon))^{-1}$ . The term  $\Sigma(\mathbf{k}, \epsilon)$  is the self-energy and contains information about the bath modes. The effective Hamiltonian  $H_{eff}(\mathbf{k})$  contains a dissipation term  $H_{diss} = i(\gamma_i \sigma_i)$ ,  $i = (0, x, y, z)$ , which makes it non-Hermitian. Non-Hermitian Hamiltonians have complex eigenvalues and distinct right and left eigenstates, demanding the use of a biorthogonal algebra [38, 39]. In the formalism of coupled baths above, the physical requirement that the system's density of states is non-negative results in a constraint to the complex eigenvalues: their imaginary part has to be non-positive [37].

Regarding the transport properties of quasiparticles, it is established that the Hall conductivity for a two-dimensional fermionic system can be obtained from the Matsubara Green function  $G$  as [17, 40, 41]:

$$\sigma_{xy} = \frac{e^2}{h} \frac{\varepsilon_{\mu\nu\rho}}{24\pi^2} \int d^3 p \text{Tr} \left[ G \frac{\partial G}{\partial p_\mu} G \frac{\partial G}{\partial p_\nu} G \frac{\partial G}{\partial p_\rho} \right] \quad (1)$$

where we assume  $T = 0 K$  so the sum over Matsubara frequencies becomes an integral. The expression above works for either Hermitian and non-Hermitian Hamiltonians, provided that the Green function is known. For a Hermitian Hamiltonian, this Hall conductivity is quantized and gives rise to the integer Hall effect. That is a consequence of the non-trivial topology of the Hamiltonian's Bloch bundle [1, 2]. The quantization is indexed by the Chern number or TKNN integer [42]. The system is a topological insulator due to the bulk-edge correspondence. However, for a non-Hermitian system, the self-energy  $\Sigma(\mathbf{k}, \epsilon)$  spoils this quantization even if the system has non-trivial Chern topology [15, 17]. In this work, this is shown explicitly in the case of the non-Hermitian checkerboard lattice.

## 3 Hermitian checkerboard lattice

To investigate the Hall conductivity of the checkerboard fermionic lattice, we begin by analyzing the Hermitian

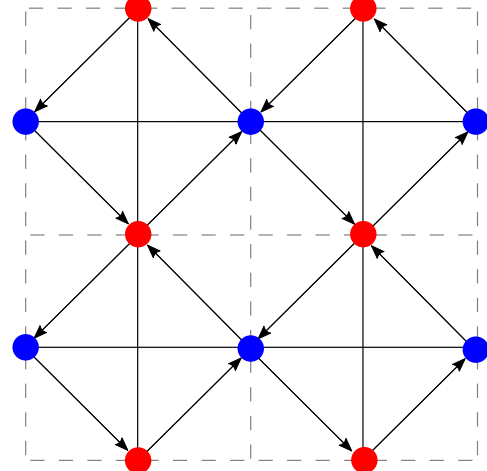


Figure 1: The checkerboard lattice. The inequivalent sites are represented in blue and red. The NN hopping is complex, with a phase of  $+\phi$  in the direction of the arrows and  $-\phi$  against it. The NNN hopping is represented by the solid vertical and horizontal lines. We chose the lattice parameter as  $a = 1$ .

case. The checkerboard lattice is represented in Figure 1, with tight-binding Hamiltonian written as:

$$H^H = -t \sum_{\langle i,j \rangle} e^{i\phi_{ij}} (c_i^\dagger c_j + h.c.) - \sum_{\langle\langle i,j \rangle\rangle} t'_{ij} (c_i^\dagger c_j + h.c.). \quad (2)$$

Here,  $c_i^\dagger (c_i)$  is the fermion creation (annihilation) operator at site  $i$ . The pairs  $\langle i,j \rangle$  and  $\langle\langle i,j \rangle\rangle$  represent near-neighbor (NN) and next-near-neighbor (NNN) sites, respectively. There are two inequivalent sites in the primitive cell. The NN hopping is complex, carrying a phase factor  $\phi_{ij} = \pm\phi$  with the sign determined by the arrows' directions in Figure 1. That term breaks the time-reversal symmetry for  $\phi \neq n\pi$  ( $n \in \mathbb{Z}$ ) and allows non-trivial topology [25]. The NNN hopping  $t'_{ij} = t'_1 (t'_2)$  is represented by solid (dashed) lines. As a minimal model, we take  $t'_2 = 0$  and call  $t'_1 = t'$ . In the momentum space we have a two-band system, and the general Hermitian Hamiltonian is:

$$H^H = \sum_k \psi_k^\dagger H_k^H \psi_k \quad (3)$$

with  $\psi^\dagger = (a_k^\dagger \ b_k^\dagger)$ . The checkerboard Hamiltonian matrix takes the form

$$H_k^H = d_0 I + d_x \sigma_x + d_y \sigma_y + d_z \sigma_z \quad (4)$$

with

$$\begin{aligned}
d_0 &= -t' (\cos k_x + \cos k_y) \\
d_x &= -4t \cos \phi \left( \cos \frac{k_x}{2} \cos \frac{k_y}{2} \right) \\
d_y &= -4t \sin \phi \left( \sin \frac{k_x}{2} \sin \frac{k_y}{2} \right) \\
d_z &= -t' (\cos k_x - \cos k_y).
\end{aligned} \tag{5}$$

The Hamiltonian's eigenvalues are

$$\epsilon_{\pm} = d_0 \pm d, \quad d \equiv \sqrt{d_x^2 + d_y^2 + d_z^2} \tag{6}$$

and the spectrum is gapped for  $\phi \neq m\pi$  ( $m \in \mathbb{Z}/2$ ).

The Berry curvature of the  $n$ -th band is a local function of the momenta constructed from the eigenstates and defined as  $\Omega_{n,ij}(\mathbf{k}) = i\varepsilon_{ij} \langle \partial_i \psi_n(\mathbf{k}) | \partial_j \psi_n(\mathbf{k}) \rangle$ . For a two-band system with Hamiltonian written as Eq. 4, the Berry curvature of the valence band can be written as [1, 2, 43]:

$$\Omega_{xy}(\mathbf{k}) = \hat{\mathbf{d}} \cdot (\partial_x \hat{\mathbf{d}} \times \partial_y \hat{\mathbf{d}}) \tag{7}$$

with  $\hat{\mathbf{d}} = \mathbf{d}/d$ ,  $\mathbf{d} = (d_x, d_y, d_z)$ . From the linear response theory, the Hall conductivity is given by:

$$\sigma_{xy} = -\frac{e^2}{h} \int \frac{d^2 k}{4\pi} \Omega_{xy}(\mathbf{k}) = -\frac{e^2}{h} C. \tag{8}$$

Here,  $C \equiv \int \frac{d^2 k}{4\pi} \Omega_{xy}(\mathbf{k})$  is the Chern number. Hence, the Hall conductivity is quantized, realizing the integer quantum Hall effect. In the case of a two-band insulator, the Chern number has a natural geometrical interpretation. As  $\mathbf{k}$  spreads over the Brillouin torus, the parameter vector  $\mathbf{d}$  describes a surface. The Chern number represents the number of times this surface wraps around the origin (the winding number).

In Hermitian systems, a non-trivial Chern number is related to robust conducting edge states via bulk-boundary correspondence, making the system a topological insulator. In the gapped checkerboard lattice, the Chern number is  $C = -1$  if  $\phi$  lays in the first and third quadrant, and  $C = +1$  for  $\phi$  in the second and fourth quadrant. For  $\phi = n\pi/2$ , the system is ungapped. The bands touch quadratically at the corners of the Brillouin zone for even  $n$ , and in the center for odd  $n$ .

## 4 Non-Hermitian case

One way of obtaining a non-Hermitian Hamiltonian is to include an anti-Hermitian diagonal term in the momentum-space Hamiltonian:

$$H^{AH} = \sum_k \psi_k^\dagger H_k^{AH} \psi_k \tag{9}$$

where

$$\begin{aligned}
H_k^{AH} &= i \begin{pmatrix} \gamma_a & 0 \\ 0 & -\gamma_b \end{pmatrix} = i \begin{pmatrix} \gamma_0 + \gamma_z & 0 \\ 0 & \gamma_0 - \gamma_z \end{pmatrix} \\
&= i(\gamma_0 I + \gamma_z \sigma_z).
\end{aligned} \tag{10}$$

Here, we defined  $\gamma_0 \equiv \frac{(\gamma_a - \gamma_b)}{2}$  and  $\gamma_z \equiv \frac{(\gamma_a + \gamma_b)}{2}$ .

The total non-Hermitian Hamiltonian  $H_k^{NH} = H_k^H + H_k^{AH}$  can be written with complex parameters  $h_i \equiv d_i + i\gamma_i$  as

$$H_k = h_0 I + h_x \sigma_x + h_y \sigma_y + h_z \sigma_z. \tag{11}$$

This is a general form. In our system, the only non-real parameters (which carry the non-Hermiticity) are  $h_0 = d_0 + i\gamma_0$  and  $h_z = d_z + i\gamma_z$ . Diagonalizing the Hamiltonian we obtain the eigenvalues:

$$\epsilon_{\pm} = h_0 \pm h \tag{12}$$

with

$$\begin{aligned}
h &= \sqrt{h_x^2 + h_y^2 + h_z^2} = \sqrt{d_x^2 + d_y^2 + (d_z + i\gamma_z)^2} \\
&= h^R + ih^I.
\end{aligned} \tag{13}$$

The eigenvalues are complex, with:

$$\begin{aligned}
Re \epsilon_{\pm} &= d_0 \pm h^R \\
Im \epsilon_{\pm} &= \gamma_0 \pm h^I.
\end{aligned} \tag{14}$$

Within the interpretation of system-environment coupling derived in Ref. [37], it is imperative that imaginary part be negative, ensuring the density of states is non-negative. To fulfill this property it is sufficient to assume  $\gamma_0 < 0$  and  $|\gamma_0| > \gamma_z$ . The spectrum is shown in Fig. 2 for different values of  $\gamma_z$ . For high values of  $\gamma_z$  the gap closes in exceptional points (EPs). Exceptional points are a unique and interesting characteristic of non-Hermitian systems. In an EP, in addition to the gap closing  $\epsilon_+ = \epsilon_-$ , the eigenvalues of the system coalesce and the Hamiltonian is said to be defective [9]. For our system, Fig. 2 shows hybrid exceptional points at  $\mathbf{k}_{HEP} = (\pm\pi/2, \pm\pi/2)$  when  $\gamma_z = 2$ . Those are called hybrid because they result from the merging of two ordinary exceptional points with opposite vorticities or winding numbers [44–46]. In fact, for  $\gamma_z > 2$ , each hybrid EP splits in two ordinary EPs localized in the  $\Gamma - M$  line. These coupled EPs are linked by a path in which the eigenvalues of both bands are complex-conjugate of each other, which is sometimes called bulk Fermi arcs [10, 47] and are a consequence of  $\mathcal{PT}$  symmetry of the Hamiltonian [11].

Another unique feature of non-Hermitian systems is the topological classification derived from the vorticity of EPs, which is related to the energy eigenvalues [44, 48]

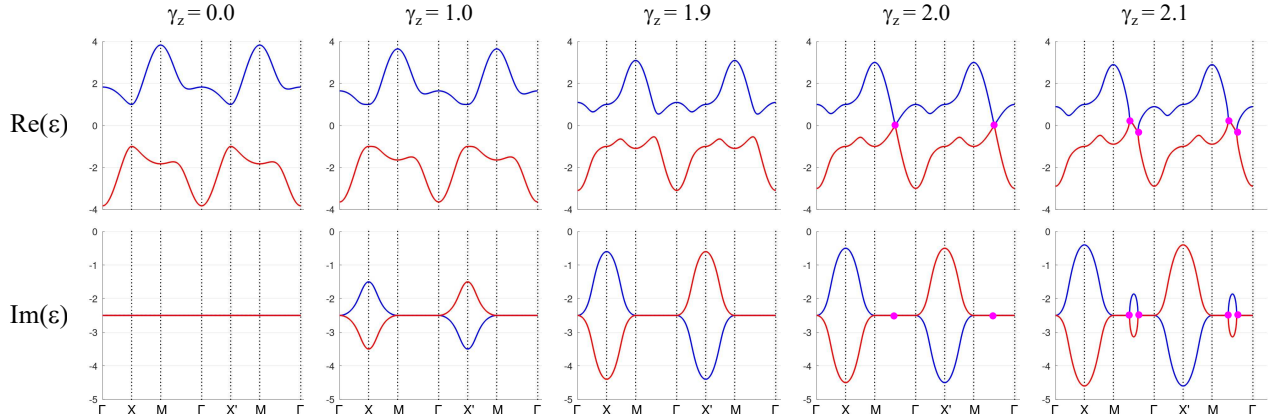


Figure 2: Energy spectrum (real and imaginary parts) of the system for different values of  $\gamma_z$ . The points of high symmetry are  $\Gamma(0, 0)$ ,  $X(\pi, 0)$ ,  $X'(\pi, \pi)$ ,  $M(\pi, \pi)$ . For  $\gamma_z = 2$ , a hybrid exceptional point (in magenta) is generated in the center of the  $\Gamma - M$  line, which splits in two ordinary EPs for  $\gamma_z > 2$ . In this work, we focus in the  $\gamma_z < 2$  regime, where the bands do not touch and the Berry curvature is well-defined. The other parameters of the theory are  $t = 1.0$ ,  $t' = 0.5$ ,  $\phi = \pi/4$ ,  $\gamma_0 = -2.5$ .

(rather than the eigenstates like in Chern or  $\mathbb{Z}_2$  insulators [1]). This classification is not the focus of the present work and is left for forthcoming studies. For the investigation of transverse transport, we restrict ourselves to the gapped regime.

## 5 Hall Conductivity

We can generalize the Berry curvature in Eq. 7 to non-Hermitian systems, obtaining a non-Hermitian complex Berry curvature [16]:

$$\Omega_{xy}(\mathbf{k}) = \hat{\mathbf{h}} \cdot (\partial_x \hat{\mathbf{h}} \times \partial_y \hat{\mathbf{h}}) \quad (15)$$

where  $\hat{\mathbf{h}} = \mathbf{h}/h$ ,  $\mathbf{h} = (h_x, h_y, h_z)$ . Actually, because of the difference between right and left eigenstates, we can construct four different ‘‘Berry curvatures’’  $\Omega_{xy}^{\alpha\beta}(\mathbf{k}) = i\varepsilon_{xy} \langle \partial_x \psi^\alpha(\mathbf{k}) | \partial_y \psi^\beta(\mathbf{k}) \rangle$ , where  $\alpha, \beta = L/R$  [44]. We use here  $\Omega_{xy}(\mathbf{k}) = \Omega_{xy}^{LR}(\mathbf{k})$ , which is well-suited for systems with loss and gain. The non-Hermitian Chern number is defined as in the Hermitian case:  $C \equiv \int \frac{d^2k}{4\pi} \Omega_{xy}^{\alpha\beta}(\mathbf{k})$ . It is a real and quantized number and does not depend on  $\alpha, \beta$ , even though  $\Omega_{xy}^{\alpha\beta}(\mathbf{k})$  are locally different.

In ordinary Hermitian systems, non-trivial Chern numbers are related to robust edge states through the bulk-edge correspondence, characterizing a topological insulator. This bulk-edge correspondence breaks down in non-Hermitian systems. It has been argued that it can be restored defining a non-Bloch Chern number as the integral of the Berry curvature over an extended complex Brillouin zone [14]. Nevertheless, the bulk Hall transport is unaffected by that. The Hall conductivity in Eq. 1 can

be written as [17]:

$$\begin{aligned} \sigma_{xy} &= -\frac{e^2}{h} \int \frac{d^2k}{2\pi^2} \text{Re} \left[ \hat{\mathbf{h}} \cdot (\hat{\mathbf{h}}_x \times \hat{\mathbf{h}}_y) \right] \times \\ &\quad \times \left( \frac{\pi}{2} \text{sgn}(\text{Re } h) - \frac{i h h_0}{h^2 - h_0^2} - i \text{arctanh} \left( \frac{h_0}{h} \right) \right) \\ &= -\frac{e^2}{h} \int \frac{d^2k}{4\pi} \text{Re} [\Omega_{xy}(\mathbf{k}) f(\mathbf{k})]. \end{aligned} \quad (16)$$

The conductivity now bears a factor  $f(\mathbf{k})$  in the integrand, and we cannot identify the integral with the Chern number. Therefore, there is no topological interpretation of the Hall response, and the Hall conductivity for a non-Hermitian topological Chern insulator is in general non-quantized. Taking the Hermitian limit  $\mathbf{h} \rightarrow \mathbf{d}$ , we can show that the expression above reduces to Eq. 8, restoring the integer quantum Hall effect.

In the insulating regime, the non-Hermitian Chern number was numerically calculated and is equal to  $C = \pm 1$ , like in the Hermitian system. The values of  $\phi$  for which the gap closes are not only  $n\pi/2$  (as in the Hermitian case), but an interval around those values. In that interval, the gap closes in exceptional points, the Berry curvature diverges and the Chern number is not defined. As long as we stay in the insulating phase, the Chern topology is identical to the Hermitian system. The real and imaginary parts of the Berry curvature are plotted in Figure 3. Note that  $\text{Im } \Omega_{xy}(\mathbf{k})$  is an odd function ( $\text{Im } \Omega_{xy}(-\mathbf{k}) = -\text{Im } \Omega_{xy}(\mathbf{k})$ ), so its integral is null, making the Chern number a real integer.

The Hall conductivity as a function of  $\gamma_z$  is plotted in Figure 4. The conductivity increases with the raise of  $\gamma_z$ , but decreases with the raise of  $|\gamma_0|$ . This is in accordance

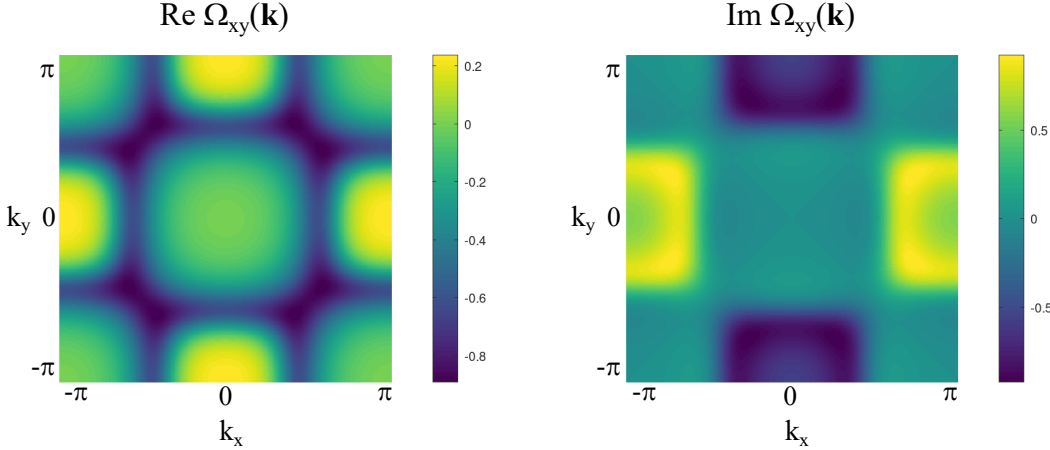


Figure 3: Berry curvature of the non-Hermitian checkerboard lattice. Parameters:  $t = 1.0$ ,  $t' = 0.5$ ,  $\phi = \pi/4$ ,  $\gamma_0 = -2.5$ .

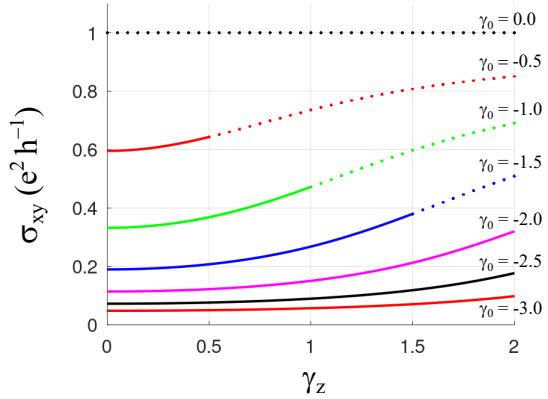


Figure 4: Hall conductivity of the non-Hermitian checkerboard lattice as a function of  $\gamma_z$ . Different curves represent different values of  $\gamma_0$ . The other parameters are  $t = 1.0$ ,  $t' = 0.5$  and  $\phi = \pi/4$ . The dotted sections of the plots are not physical in the coupled baths model ( $\gamma_z > |\gamma_0|$ ). The data does not go further than  $\gamma_z = 2.0$  because this is the value of gap closing, where the Berry curvature is divergent.

with the interpretation that, for systems coupled to the environment,  $|\gamma_0| > \gamma_z$  represent a net loss, i.e., particles with finite lifetimes [39]. A high value of  $|\gamma_0|$  means higher loss (or shorter quasiparticle lifetime), decreasing the charge carriers in equilibrium and damping the conductivity. The opposite occurs for a high  $\gamma_z$ , which means longer quasiparticle lifetime (less loss), resulting in a higher conductivity.

## 6 Summary and concluding remarks

We studied the fermionic non-Hermitian checkerboard lattice with focus on its Chern topology and Hall conductivity. The non-Hermiticity is introduced by two parameters:  $\gamma_0$ , related to dissipation, and  $\gamma_z$ , related to gain. A complex NN hopping induces a Berry curvature, which renders the system a non-trivial Chern topology in the insulating phase (identically to the Hermitian case). The gap closes in exceptional points for some choices of parameters, in specific for high  $\gamma_z$ . Although the system is a Chern insulator, the Hall conductivity is not quantized. This is a consequence of dissipation or finite lifetime of states in a context of a system coupled to the environment. We verified the response of the Hall conductivity to the non-Hermitian parameters, and concluded it is maximized for high  $\gamma_z$  and low  $\gamma_0$ , which represents long quasiparticle lifetimes. Our work explores the novel field of non-Hermitian topology and corroborates that two-dimensional exotic lattices, like the checkerboard lattice, can be a good platform to investigate topological effects in open quantum systems.

## References

- [1] M. Z. Hasan, C. L. Kane, Colloquium: Topological insulators, Rev. Mod. Phys. 82 (4) (2010) 3045–3067. doi:10.1103/revmodphys.82.3045. URL <http://dx.doi.org/10.1103/RevModPhys.82.3045>
- [2] M. Fruchart, D. Carpentier, An introduction to topological insulators, C. R. Phys. 14 (9–10) (2013) 779–815. doi:10.1016/j.crhy.2013.09.013.

- URL <http://dx.doi.org/10.1016/j.crhy.2013.09.013>
- [3] S. Ryu, A. P. Schnyder, A. Furusaki, A. W. W. Ludwig, Topological insulators and superconductors: tenfold way and dimensional hierarchy, *New J. Phys.* 12 (6) (2010) 065010. doi:10.1088/1367-2630/12/6/065010. URL <http://dx.doi.org/10.1088/1367-2630/12/6/065010>
- [4] X.-L. Qi, S.-C. Zhang, Topological insulators and superconductors, *Rev. Mod. Phys.* 83 (4) (2011) 1057–1110. doi:10.1103/revmodphys.83.1057. URL <http://dx.doi.org/10.1103/RevModPhys.83.1057>
- [5] R. Süssstrunk, S. D. Huber, Observation of phononic helical edge states in a mechanical topological insulator, *Science* 349 (6243) (2015) 47–50. doi:10.1126/science.aab0239. URL <http://dx.doi.org/10.1126/science.aab0239>
- [6] N. Goldman, J. C. Budich, P. Zoller, Topological quantum matter with ultracold gases in optical lattices, *Nature Phys.* 12 (7) (2016) 639–645. doi:10.1038/nphys3803. URL <http://dx.doi.org/10.1038/nphys3803>
- [7] T. Ozawa, H. M. Price, A. Amo, N. Goldman, M. Hafezi, L. Lu, M. C. Rechtsman, D. Schuster, J. Simon, O. Zilberberg, I. Carusotto, Topological photonics, *Rev. Mod. Phys.* 91 (1) (Mar. 2019). doi:10.1103/revmodphys.91.015006. URL <http://dx.doi.org/10.1103/RevModPhys.91.015006>
- [8] M. Malki, G. S. Uhrig, Topological magnetic excitations, *EPL* 132 (2) (2020) 20003. doi:10.1209/0295-5075/132/20003. URL <http://dx.doi.org/10.1209/0295-5075/132/20003>
- [9] Y. Ashida, Z. Gong, M. Ueda, Non-Hermitian physics, *Adv. Phys.* 69 (3) (2020) 249–435. doi:10.1080/00018732.2021.1876991. URL <http://dx.doi.org/10.1080/00018732.2021.1876991>
- [10] T. Tlusty, Exceptional topology in ordinary soft matter, *Phys. Rev. E* 104 (2) (Aug. 2021). doi:10.1103/physreve.104.025002. URL <http://dx.doi.org/10.1103/PhysRevE.104.025002>
- [11] H. M. Hurst, B. Flebus, Non-Hermitian physics in magnetic systems, *J. Appl. Phys.* 132 (22) (Dec. 2022). doi:10.1063/5.0124841. URL <http://dx.doi.org/10.1063/5.0124841>
- [12] A. Banerjee, R. Sarkar, S. Dey, A. Narayan, Non-Hermitian topological phases: principles and prospects, *J. Phys.: Condens. Matter* 35 (33) (2023) 333001. doi:10.1088/1361-648x/acd1cb. URL <http://dx.doi.org/10.1088/1361-648X/acd1cb>
- [13] T. Yu, J. Zou, B. Zeng, J. Rao, K. Xia, Non-Hermitian topological magnonics, *Phys. Rep.* 1062 (2024) 1–86. doi:10.1016/j.physrep.2024.01.006. URL <http://dx.doi.org/10.1016/j.physrep.2024.01.006>
- [14] S. Yao, F. Song, Z. Wang, Non-Hermitian Chern bands, *Phys. Rev. Lett.* 121 (13) (Sep. 2018). doi:10.1103/physrevlett.121.136802. URL <http://dx.doi.org/10.1103/PhysRevLett.121.136802>
- [15] M. Hirschberger, R. Chisnell, Y. S. Lee, N. P. Ong, Thermal Hall effect of spin excitations in a kagome magnet, *Phys. Rev. Lett.* 115 (2015) 106603. doi:10.1103/PhysRevLett.115.106603. URL <https://link.aps.org/doi/10.1103/PhysRevLett.115.106603>
- [16] Y. Chen, H. Zhai, Hall conductance of a non-Hermitian Chern insulator, *Phys. Rev. B* 98 (24) (Dec. 2018). doi:10.1103/physrevb.98.245130. URL <http://dx.doi.org/10.1103/PhysRevB.98.245130>
- [17] M. R. Hirsbrunner, T. M. Philip, M. J. Gilbert, Topology and observables of the non-Hermitian Chern insulator, *Phys. Rev. B* 100 (8) (Aug. 2019). doi:10.1103/physrevb.100.081104. URL <http://dx.doi.org/10.1103/PhysRevB.100.081104>
- [18] B. Canals, From the square lattice to the checkerboard lattice: Spin-wave and large-n limit analysis, *Phys. Rev. B* 65 (18) (Apr. 2002). doi:10.1103/physrevb.65.184408. URL <http://dx.doi.org/10.1103/PhysRevB.65.184408>
- [19] S. Fujimoto, Geometrical-frustration-induced (semi)metal-to-insulator transition, *Phys. Rev. Lett.* 89 (2002) 226402. doi:10.1103/PhysRevLett.89.226402. URL <https://link.aps.org/doi/10.1103/PhysRevLett.89.226402>
- [20] J.-S. Bernier, C.-H. Chung, Y. B. Kim, S. Sachdev, Planar pyrochlore antiferromagnet: A large- $N$  analysis, *Phys. Rev. B* 69 (21) (Jun. 2004). doi:10.1103/physrevb.69.214427. URL <http://dx.doi.org/10.1103/PhysRevB.69.214427>

- [21] F. Pollmann, J. J. Betouras, K. Shtengel, P. Fulde, Correlated fermions on a checkerboard lattice, Phys. Rev. Lett. 97 (17) (Oct. 2006). doi:10.1103/physrevlett.97.170407.  
URL <http://dx.doi.org/10.1103/PhysRevLett.97.170407>
- [22] T. Yoshioka, A. Koga, N. Kawakami, Frustration effects in an anisotropic checkerboard lattice Hubbard model, Phys. Rev. B 78 (2008) 165113. doi:10.1103/PhysRevB.78.165113.  
URL <https://link.aps.org/doi/10.1103/PhysRevB.78.165113>
- [23] E. G. Santos, J. R. Iglesias, C. Lacroix, M. A. Gusmão, A two-band model for superconductivity in the checkerboard lattice, J. Phys.: Condens. Matter 22 (21) (2010) 215701. doi:10.1088/0953-8984/22/21/215701.  
URL <https://dx.doi.org/10.1088/0953-8984/22/21/215701>
- [24] K. Sun, H. Yao, E. Fradkin, S. A. Kivelson, Topological insulators and nematic phases from spontaneous symmetry breaking in 2d fermi systems with a quadratic band crossing, Phys. Rev. Lett. 103 (2009) 046811. doi:10.1103/PhysRevLett.103.046811.  
URL <https://link.aps.org/doi/10.1103/PhysRevLett.103.046811>
- [25] K. Sun, Z. Gu, H. Katsura, S. Das Sarma, Nearly flatbands with nontrivial topology, Phys. Rev. Lett. 106 (23) (Jun. 2011). doi:10.1103/physrevlett.106.236803.  
URL <http://dx.doi.org/10.1103/PhysRevLett.106.236803>
- [26] H. Katsura, I. Maruyama, A. Tanaka, H. Tasaki, Ferromagnetism in the Hubbard model with topological/non-topological flat bands, Europhys. Lett. 91 (5) (2010) 57007. doi:10.1209/0295-5075/91/57007.  
URL <http://dx.doi.org/10.1209/0295-5075/91/57007>
- [27] H. Liu, G. Sethi, S. Meng, F. Liu, Orbital design of flat bands in non-line-graph lattices via line-graph wave functions, Phys. Rev. B 105 (8) (Feb. 2022). doi:10.1103/physrevb.105.085128.  
URL <http://dx.doi.org/10.1103/PhysRevB.105.085128>
- [28] X.-P. Liu, Y. Zhou, Y.-F. Wang, C.-D. Gong, Characterizations of topological superconductors: Chern numbers, edge states and Majorana zero modes, New J. Phys. 19 (9) (2017) 093018. doi:10.1088/1367-2630/aa8022  
URL <http://dx.doi.org/10.1088/1367-2630/aa8022>
- [29] A. Pires, Magnon spin Nernst effect on the antiferromagnetic checkerboard lattice, Phys. Lett. A 383 (32) (2019) 125887. doi:10.1016/j.physleta.2019.125887.  
URL <http://dx.doi.org/10.1016/j.physleta.2019.125887>
- [30] A. S. T. Pires, Topological magnons in the antiferromagnetic checkerboard lattice, Physica E 118 (2020) 113899. doi:10.1016/j.physe.2019.113899.  
URL <https://doi.org/10.1016/j.physe.2019.113899>
- [31] A. Pires, Topological magnons on the checkerboard lattice, Physica B 602 (2021) 412490. doi:10.1016/j.physb.2020.412490.  
URL <http://dx.doi.org/10.1016/j.physb.2020.412490>
- [32] D.-S. Ma, Y. Xu, C. S. Chiu, N. Regnault, A. A. Houck, Z. Song, B. A. Bernevig, Spin-orbit-induced topological flat bands in line and split graphs of bipartite lattices, Phys. Rev. Lett. 125 (2020) 266403. doi:10.1103/PhysRevLett.125.266403.  
URL <https://link.aps.org/doi/10.1103/PhysRevLett.125.266403>
- [33] Z. Zhang, W. Feng, Y. Yao, B. Tang, Photoinduced Floquet topological magnons in a ferromagnetic checkerboard lattice, Phys. Lett. A 414 (2021) 127630. doi:10.1016/j.physleta.2021.127630.  
URL <http://dx.doi.org/10.1016/j.physleta.2021.127630>
- [34] H. Kabbour, E. Janod, B. Corraze, M. Danot, C. Lee, M.-H. Whangbo, L. Cario, Structure and magnetic properties of oxychalcogenides  $A_2F_2Fe_2OQ_2$  ( $A = Sr, Ba$ ;  $Q = S, Se$ ) with  $Fe_2O$  square planar layers representing an antiferromagnetic checkerboard spin lattice, J. Am. Chem. Soc. 130 (26) (2008) 8261–8270. doi:10.1021/ja711139g.  
URL <http://dx.doi.org/10.1021/ja711139g>
- [35] X. Hu, R.-W. Zhang, D.-S. Ma, Z. Cai, D. Geng, Z. Sun, Q. Zhao, J. Gao, P. Cheng, L. Chen, K. Wu, Y. Yao, B. Feng, Realization of a two-dimensional checkerboard lattice in monolayer  $Cu_2N$ , Nano Lett. 23 (12) (2023) 5610–5616. doi:10.1021/acs.nanolett.3c01111.  
URL <http://dx.doi.org/10.1021/acs.nanolett.3c01111>
- [36] A. Sufyan, M. Sajjad, J. Andreas Larsson, Evaluating the potential of planar checkerboard lattice

- Cu<sub>2</sub>N* monolayer as anode material for lithium and sodium-ion batteries using first-principles methods, *Appl. Surf. Sci.* 654 (2024) 159474. doi:10.1016/j.apsusc.2024.159474. URL <http://dx.doi.org/10.1016/j.apsusc.2024.159474>
- [37] J. M. Midtgård, Z. Wu, Y. Chen, Constraints on the energy spectrum of non-Hermitian models in open environments, *Eur. Phys. J. B* 92 (11) (Nov. 2019). doi:10.1140/epjb/e2019-100393-5. URL <http://dx.doi.org/10.1140/epjb/e2019-100393-5>
- [38] D. C. Brody, Biorthogonal quantum mechanics, *J. Phys. A: Math. Theor.* 47 (3) (2013) 035305. doi:10.1088/1751-8113/47/3/035305. URL <http://dx.doi.org/10.1088/1751-8113/47/3/035305>
- [39] S. Groenendijk, T. L. Schmidt, T. Meng, Universal Hall conductance scaling in non-Hermitian Chern insulators, *Phys. Rev. Res.* 3 (2) (Apr. 2021). doi:10.1103/physrevresearch.3.023001. URL <http://dx.doi.org/10.1103/PhysRevResearch.3.023001>
- [40] K. Ishikawa, T. Matsuyama, Magnetic field induced multi-component  $QED_3$  and quantum Hall effect, *Z. Phys. C - Particles and Fields* 33 (1) (1986) 41–45. doi:10.1007/bf01410451. URL <http://dx.doi.org/10.1007/BF01410451>
- [41] K. Ishikawa, T. Matsuyama, A microscopic theory of the quantum Hall effect, *Nucl. Phys. B* 280 (1987) 523–548. doi:10.1016/0550-3213(87)90160-x. URL [http://dx.doi.org/10.1016/0550-3213\(87\)90160-X](http://dx.doi.org/10.1016/0550-3213(87)90160-X)
- [42] D. J. Thouless, M. Kohmoto, M. P. Nightingale, M. den Nijs, Quantized Hall conductance in a two-dimensional periodic potential, *Phys. Rev. Lett.* 49 (6) (1982) 405–408. doi:10.1103/physrevlett.49.405. URL <https://doi.org/10.1103/physrevlett.49.405>
- [43] A. S. T. Pires, A brief introduction to topology and differential geometry in condensed matter physics, IOP Concise Physics, Morgan & Claypool, San Rafael, CA, 2019.
- [44] H. Shen, B. Zhen, L. Fu, Topological band theory for non-Hermitian Hamiltonians, *Phys. Rev. Lett.* 120 (14) (Apr. 2018). doi:10.1103/physrevlett.120.146402. URL <http://dx.doi.org/10.1103/PhysRevLett.120.146402>
- [45] X.-L. Zhang, C. T. Chan, Hybrid exceptional point and its dynamical encircling in a two-state system, *Phys. Rev. A* 98 (3) (Sep. 2018). doi:10.1103/physreva.98.033810. URL <http://dx.doi.org/10.1103/PhysRevA.98.033810>
- [46] L. Jin, H. C. Wu, B.-B. Wei, Z. Song, Hybrid exceptional point created from type-iii Dirac point, *Phys. Rev. B* 101 (4) (Jan. 2020). doi:10.1103/physrevb.101.045130. URL <http://dx.doi.org/10.1103/PhysRevB.101.045130>
- [47] H. Zhou, C. Peng, Y. Yoon, C. W. Hsu, K. A. Nelson, L. Fu, J. D. Joannopoulos, M. Soljačić, B. Zhen, Observation of bulk Fermi arc and polarization half charge from paired exceptional points, *Science* 359 (6379) (2018) 1009–1012. doi:10.1126/science.aap9859. URL <http://dx.doi.org/10.1126/science.aap9859>
- [48] S. Dey, A. Banerjee, D. Chowdhury, A. Narayan, Hall conductance of a non-Hermitian Weyl semimetal, *New J. Phys.* 26 (2) (2024) 023057. doi:10.1088/1367-2630/ad2b0e. URL <http://dx.doi.org/10.1088/1367-2630/ad2b0e>